Optical microfiber-based photonic crystal cavity

Yi-zhi Sun[1,3], Yang Yu[2], Hui-lan Liu[1], Zhi-yuan Li[2] and Wei Ding[2,3]
[1]School of Instrumentation Science and Opto-electronics Engineering, Beihang University, Beijing 100191, China
[2]Laboratory of Optical Physics, Institute of Physics, Chinese Academy of Sciences, Beijing 100190, China

E-mail: 375816019@qq.com, wding@iphy.ac.cn

Abstract. Using a focused ion beam milling technique, we fabricate broad stop band (~10% wide) photonic crystal (PhC) cavities in adiabatically-tapered silica fibers. Abrupt structural design of PhC mirrors efficiently reduces radiation loss, increasing the cavity finesse to ~7.5. Further experiments and simulations verify that the remaining loss is mainly due to Ga ion implantation. Such a microfiber PhC cavity probably has potentials in many light-matter interaction applications.

1. Introduction

Efficient coupling of light to subwavelength structures (either quantum emitters or dielectric particles) recently attracts great interests in fields ranging from quantum information science [1], to nonlinear optics [2], and to biochemical sensing [3]. Tightly confining light to small volume, as various optical microcavities pursue [4], is the key issue. In such a context, a tapered silica fiber enclosed by two mirrors exhibits great virtues because of moderate refractive index of silica and fabrication superiority of fiber taper. Firstly, the refractive index of silica is low enough for allowing intense evanescent field to spread out across silica boundary. Such a tapered fiber is usually referred to as micro/nano-fiber [5]. Secondly, refractive index of silica is also large enough not only for providing tight transverse field confinement but also for shortening cavity length in the longitudinal direction. For the former, when the guided mode of a tapered fiber is shrunk to the order of wavelength square, efficient light-particle interaction inside a cavity does not rely on ultra-high-finesse mirrors any more [6]. For the latter, if the index contrast between silica and air is efficiently exploited, rather than being shallowly utilized [7], penetration depth in the photonic crystal (PhC) mirror in a microfiber can be substantially shortened with the increase of its stop band [8]. Thirdly, thanks to the maturity of fiber tapering technique, the linkage between microfiber cavity and external optical network can be created conveniently and with low loss. Surface of silica fiber keeps atomically smooth during fiber tapering, and adiabatic taper transition can efficiently eliminate in-coupling and out-coupling losses. Lastly but not least, different from other on-chip photonic wires [9], a tapered fiber can maintain free-suspension configuration, which is flexible for many practical applications.

Achieving all these merits in a single device is a big challenge because of both optical and mechanical reasons. Compared with higher-index semiconductor waveguides [10], PhC structures in a silica fiber taper will produce much higher radiation loss, undermining cavity finesse. To elucidate this

[3] To whom any correspondence should be addressed.

radiation generation process, we had developed an analytical model and found that significant part of radiation light could be suppressed and recycled via an interferometric means [11]. This radiation suppression effect was later verified in experiment [8] and inspired us to envision deploying high-reflection, short-penetration-depth microfiber PhC mirrors on both ends of a central nanofiber cavity. Our experiment also verifies that a micron-meter-sized silica fiber has sufficient mechanical strength to survive after being perforated, which is not feasible in a nanometer-sized fiber. Therefore, in an ideal situation, the envisaged fiber taper cavity has no mechanical problem and will simultaneously possess the following 4 advantages: substantial evanescent field spread outside the central nanofiber; two short but adiabatic taper transition sections connecting the central nanofiber and the extremity microfibers; tightly compressed cavity mode volume in both lateral and longitudinal directions; sufficient mechanical strength for free-suspension configuration. In contrast, two recently reported nanofiber microcavities cannot eliminate long penetration tails in their mirror sections (either nanofiber Bragg grating [12] or conventional fiber Bragg grating [13]). Intrinsically limited by mechanical strength and UV-photosensitivity technique, broad band PhC mirror in a nanofiber or in a conventional fiber is not feasible, disabling small mode volumes in such fiber taper cavities. In another work, although authors exhibit the minimal mode volume in a microfiber cavity, the fiber was buried in a layer of polymer for mechanical support [14]. As a result, the free-suspension configuration is lost.

In this work, ignoring the central nanofiber cavity temporarily, we focus our study on the design, fabrication, and characterization of PhC cavity in a freely-suspended microfiber. Investigations are expected to answer the possibility of the scheme proposed above, to test the fabrication technique, and to elucidate physical origins of the problems appearing in practical implementations.

2. Design of microfiber PhC cavity

A microfiber PhC cavity is schematically illustrated in Figure 1(a). We design a resonance at $\lambda_0 = 1.53$ μm, and the fiber diameter is set to be 1.7 μm. Without specially mentioned, in the following, we fix the refractive index of silica to be 1.444 with no dispersion. Firstly, the PhC mirror sections can be split to individual microfiber segment as shown in the inset of Figure 1(a). In each segment, an etched rectangular through-hole with the dimension of $t \times 1.2$ μm lies in the middle, longitudinal pitch of the microfiber segment is Λ, and Bloch boundaries [the green planes in Figure 1(a)] are applied on the two facets. We allow the two innermost microfiber segments to vary with their parameters t and Λ. The whole PhC cavity is symmetric with respect to its center. Secondly, using Bloch boundary conditions, we quickly calculate wavevector diagram of each microfiber segment as Figure 1(b) shows, in which a stop band appears under the air light cone (the pink line), and the middle of the stop band is kept at λ_0 by tuning the pitch Λ. Figure 1(c) plots the variations of the stop band and the pitch length as a function of the etch hole thickness t. Thirdly, choosing parameters of Figure 1(c), we can compose a whole cavity structure with $N = 9$, $t3 = 300$ nm, and $L_{cav} = 50$ μm, leaving $t1$ and $t2$ varied. All the geometrical parameters and the polarization direction have been defined in Figure 1(a), and our previous paper [11] has described this design procedure in detail.

Using finite-difference time-domain (FDTD) simulation with excitation of an internal dipole source, we obtain quality factor of the cavity (defined as $Q = \omega_0 \frac{\text{Energy stored}}{\text{Power loss}}$) as a function of $t1$ and $t2$. The maximum Q-factor appears at $t1/t2 \approx 200/100$ nm, which represents a reversely varied structure, rather than a gradually varied structure ($t1 < t2$) which is predicted by conventional impedance-matching picture [15]. It is therefore manifest that an interferometric effect plays an important role in the radiation generation and suppression process [11]. More importantly, simulation shows a finesse value of ~80 (defined as $\Im = Q \frac{\text{Free Spectral Range}}{\text{Cavity Frequency}}$), which is believed enough for many cavity quantum electrodynamics applications [6].

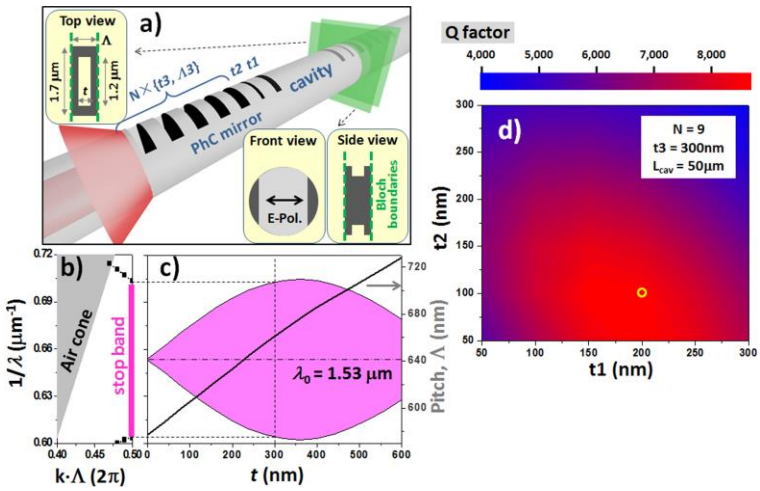

Figure 1. (a) Illustration of a microfiber PhC cavity. Individual microfiber segment is defined in the inset. (b) Wavevector diagram of one microfiber segment under Bloch boundary condition. The electric polarization is denoted in (a). (c) Stop band and pitch length as a function of the hole thickness. (d) Simulated Q-factor with variations of *t1* and *t2*.

To verify above results, we carry out another FDTD simulation by sending an optical pulse into the cavity [the red arrow in Figure 1(a)]. Normalized transmission and reflection spectra are presented in Figure 2(a). Q-factor can be read out from the spectra, $Q = \lambda_0 / \Delta\lambda$, agreeing well with the result in Figure 1(d), where $\Delta\lambda$ is the full width at half-maximum. Figure 2(a) also shows the reflectance spectra of the single PhC mirror at the two incidence directions. At the resonant wavelength 1.53 μm, a higher reflectance is observed when radiation suppression effect of PhC mirror acts. Additionally, Figure 2(b) compares the simulated spectra at the two incidence polarizations, indicating that our microfiber PhC cavity has small polarization dependence in terms of resonance wavelength. In contrast, the works based on nanofiber cavity [12, 13] exhibit much greater polarization dependence.

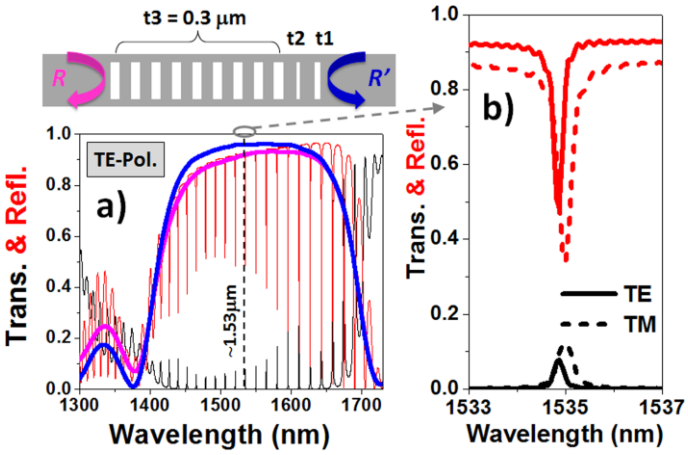

Figure 2. (a) Simulated transmittance and reflectance spectra of a microfiber PhC cavity with *t1*= 200 nm and *t2*=100 nm. Reflectance's of the single PhC mirror at different incidence directions are also shown. (b) Comparison of the reflectance spectra of the cavity at the two different polarizations.

3. Fabrication and characterization

3.1. Long cavity

In order to fabricate above devices, we adopt adiabatic fiber tapering and focused Ga ion beam (FIB) milling techniques. A scanning electron microscope (SEM) image of a microfiber PhC mirror is shown in the inset of Figure 3(a). Microfiber was firstly gently adsorbed on a flat silicon wafer via Van der Waals bonding, which allowed fixture of fiber during focused ion beam milling and detachment of fiber after fabrication. As a conducting substrate, the n-type silicon wafer also undertook the role of charge leakage. Our microfiber-based fabrication can be implemented in normal

optical room environment. In contrast, maintaining extremely clean environment is essential in nanofiber fabrication. Thanks to the dust-contamination resistance capability, our subsequent spectrum measurement to a microfiber device could be more reliable and repeatable.

To measure the transmission and reflection, a broadband fiber-based superluminescence light emitting diodes (SLED), an in-line optical circulator, and an optical spectrum analyzer were used. As shown in Fig. 3(b), we splice a passive fiber depolarizer [16, 17] after SLED source to eliminate polarization fluctuation. We also tested using in-line polarizer and polarization controller in our setup, but it is hard to resolve different polarization states in experiment. Figure 3(c) shows the measured transmittance and reflectance with a spectral resolution of 0.2 nm under unpolarised condition. The spectra can be interpreted by a Fabry-Perot picture [15], which relates Q-factor with the mirror reflectance in the inner side, r, $Q = r^{1/2}(1-r)^{-1}k_0 n_g (L_{cav} + 2L_p)$, where n_g is the group index of the guided mode, L_p is the penetration depth into the mirrors, and Q can be read out from the dips in the reflection spectrum. All of n_g, L_{cav}, and L_p can be calculated from the geometrical parameters, the Q-factor is therefore only determined by r. On the other hand, the reflectance of the same PhC mirror in its outer side (labeled R) can be estimated from the envelope of the spectrum.

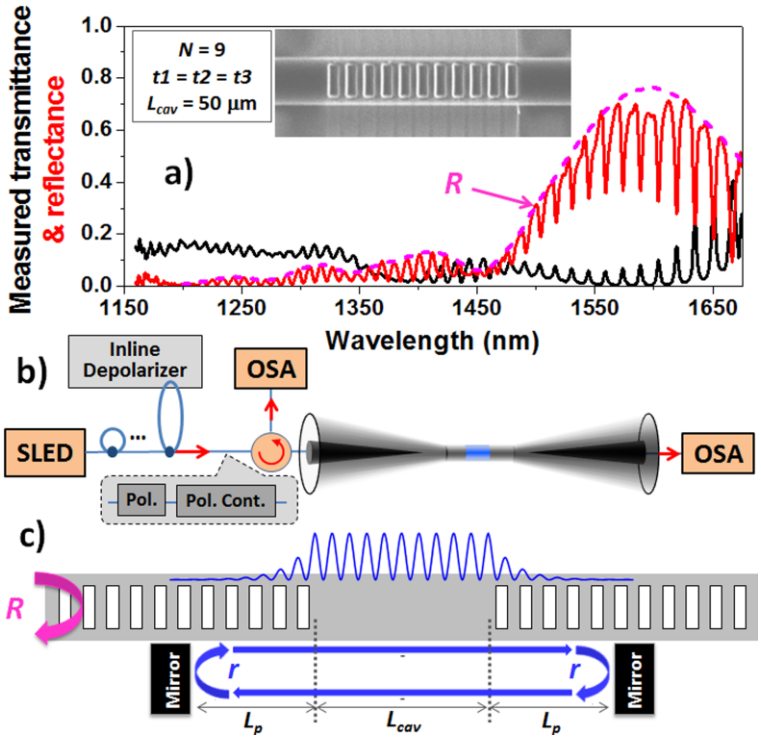

Figure 3. (a) Measured transmittance and reflectance spectra of a microfiber PhC cavity with L_{cav} = 50 µm and two PhC mirrors each having 11 etched holes (t = 300 nm). The pink dashed line is a guide to the eye and represents the reflectance envelope. Inset: SEM image of a PhC mirror. (b) Schematic of our measurement setup. (c) Fabry-Perot picture of the microfiber cavity.

Using the analysis method described above, we compare the inner and outer reflectances of a single PhC mirror without influence from fabrication variations between different devices. To test this idea, we fabricated three microfiber cavities with their geometries respectively illustrated in Figure 4. The Q-factors read out from the measured spectra are compared with the deduced Q-factors, which are derived from envelopes of reflectance. It is manifest that a gradually varied PhC mirror ($t1$ = 100 nm, $t2$ = 200 nm, $t3$ = 300 nm) can suppress radiation loss [Figure 4(b)], but, a reversely varied PhC mirror ($t1$ = 200 nm, $t2$ = 100 nm, $t3$ = 300 nm) suppress radiation more substantially [Figure 4(c)]. As a result, the inner reflectivity in Figure 4(c) is the maximum one because of the most efficient radiation suppression. All the comparisons agree well with the simulation of Figure 1(d) and can be interpreted

by our theory [11]. Note that, in obtaining results of Figure 4, we insert the in-line polarizer and polarization controller in our measurement setup.

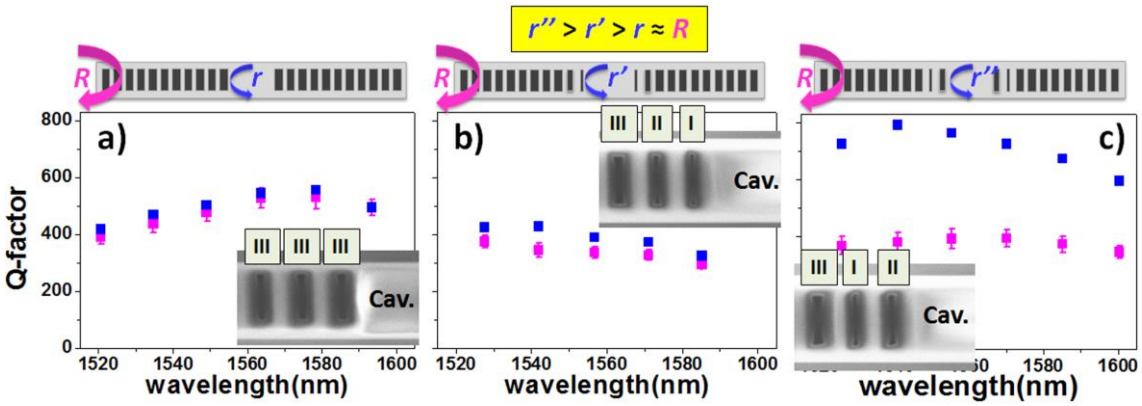

Figure 4. Measured Q-factors from reflection spectra (blue squares) and deduced Q-factors from envelopes of reflectance (pink squares) of three microfiber PhC cavities. Symbol I, II, III represent etched microfiber segments with t = 100/200/300 nm, respectively. SEM images and schematics of these three devices are depicted in the insets of (a), (b), (c).

However, our experimentally measured Q-factor (~800), hence cavity finesse (~7.5), is only one tenth of the theoretically predicted value. To find out physical origins of reminding cavity loss is our next task (see below).

3.2. Short cavity

In above analysis, we regard microfiber structure to be ideal, i.e. the geometry is symmetric and the material is pure silica. As we have pointed out [8], after FIB milling, the etched holes in microfiber cannot be vertical, and the inner walls have a tilt angle of ~9^{o}. However, taking into account this nonideality in FDTD simulation cannot fully explain the newly added cavity loss. To elucidate this problem, we study a micron-meter long cavity whose spectral details should be manifested more clearly than a macroscale cavity because of much sparser spectral distribution. Figure 5(a) shows the SEM image at tilt and normal view angles, indicating a good fabrication with center-to-center distance of the center two etched holes of 1.02 μm. Transmittance and reflectance spectra as shown in Figure 5(b) are measured under nonpolarized condition. In simulation, we assume a non-zero imaginary part (κ) of refractive index for silica material. It is seen that, when κ is set to be 0.004 [Figure 5(d)], the simulated spectra fit well with the measured spectra with respect to both magnitude and shape. The Q-factor agrees with the experimental value as well. This result implies that silica material of microfiber has been modified during FIB milling.

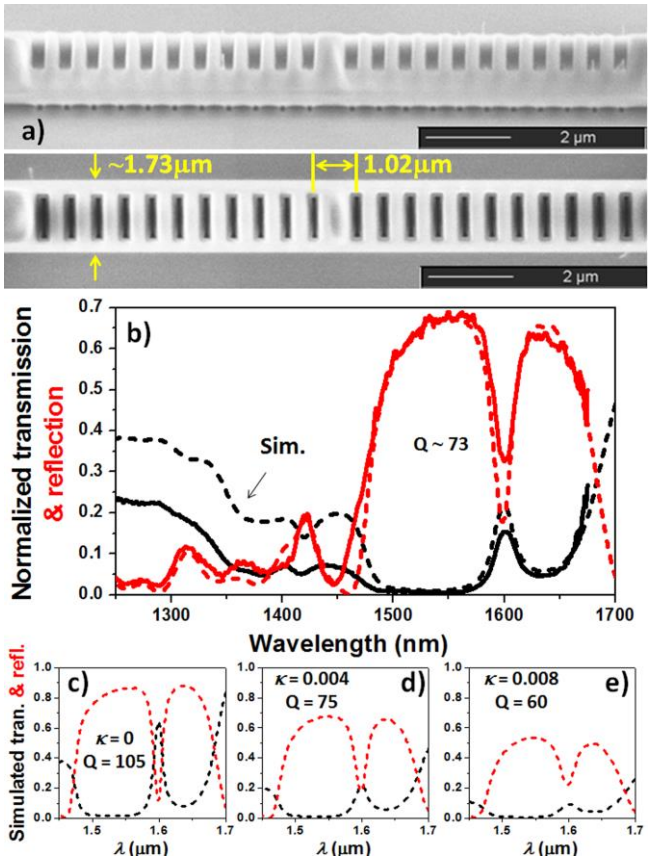

Figure 5. (a) SEM images of a microfiber PhC cavity with micron-meter cavity length. (b) Measured and simulated transmittance and reflectance spectra. (c), (d), (e) Simulations under assumptions of different imaginary parts of silica refractive index (κ), respectively. For both experiment and simulation, input sources are assumed to be unpolarised.

3.3. Ga ion contamination

It is known that Ga ion implantation in silica, which cannot be avoided in our fabrication, can cause significant loss. This may be the main origin of the above material loss. To test it, we expose different doses of Ga ions into bare microfibers, as illustrated in the inset of Figure 6, and then measure their insertion losses. Figure 6 shows an increased imaginary part of the effective modal index, $\kappa_{eff} = -\ln T \cdot (2k_0 L)^{-1}$, where T is the transmittance, L is the microfiber length having Ga ion implantation, and k_0 is the vacuum wavevector. We also present in Figure 6 the calculated k_{eff} based on the data in Reference [18]. Ga ions are assumed to concentrate in the surface layer of about 50 nm depth and overlap with the fundamental mode profile. All the curves in Figure 6 indicate that the inclusion of 0.004 into the imaginary part of silica refractive index in Figure 5 is reasonable and may be due to Ga ion contamination. We therefore conjecture that some newly appearing ion beam milling technology, such as Helium ion beam milling [19], may improve performance of microfiber PhC cavity in the future.

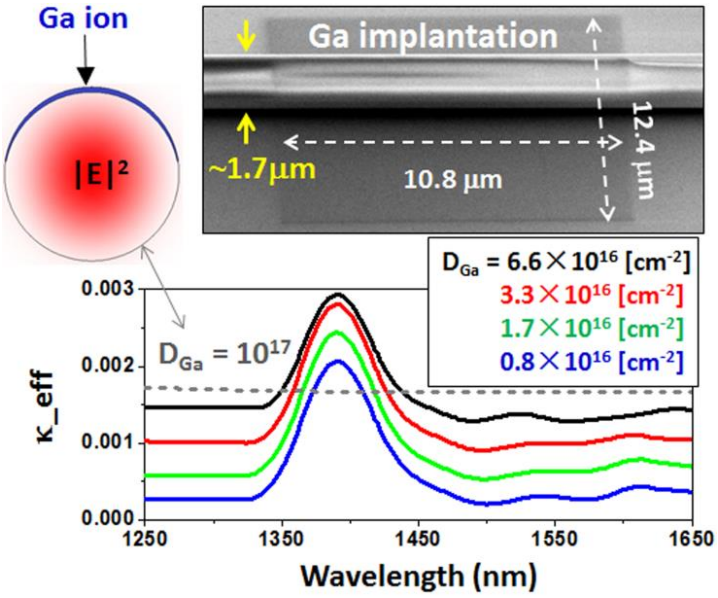

Figure 6. Measured imaginary part of the effective modal index of Ga ion contaminated microfiber. Different colours represent different Ga ion exposure doses. The peaks around 1.4 μm are due to water absorption. The grey curve is calculated based on the data in Reference [18] and fundamental modal profile.

4. Discussion and Conclusion

In summary, in an adiabatically-tapered optical fiber with diameter of a few microns, we achieve tight light confinement in PhC cavities. Our devices realize broad PhC stop bands ($\Delta\lambda/\lambda \sim 10\%$) and modest cavity finesse ($\Im \sim 7.5$) in the most popularly used optical waveguide, i.e. silica fiber. The inherent merits of silica tapered optical fibers for applications, e.g. seamless connection with conventional fiber network, excellent transparency in visible and near-infrared region, substantial evanescent field spread into environment, etc, make light confinement in microfiber of critical importance.

We present a PhC mirror design to efficiently suppress radiation loss. Also, we identify that the remaining loss in PhC cavity is the material loss caused by Ga ion implantation. Eliminating this loss may increase cavity finesse greatly. Our explorations to microfiber based PhC devices may inspire great number of interests in light-matter interaction research.

Acknowledgments

This work was supported by the National Natural Science Foundation of China (No. 61275044, 61575218, and 11204366), the Instrument Developing Project of the Chinese Academy of Sciences (No. YZ201346).

5. References

[1] Claudon J, Bleuse J, Malik N S, Bazin M, Jaffrennou P, Gregersen N, Sauvan C, Lalanne P and Gérard J- M 2010 *Nature Photonics* **4** 174
[2] Belotti M, Galli M, Gerace D, Andreani L C, Guizzetti G, Md Zain A R, Johnson N P, Sorel M and De La Rue R M 2009 *Opt. Express* **18** 1450
[3] Foreman M R, Swaim J D, and Vollmer F 2015 *Adv. Opt. Photon.* **7** 632
[4] Vahala K J 2003 *Nature* **424** 839
[5] Wu X-Q and Tong L-M 2013 *Nanophotonics* **2** 407
[6] Le Kien F and Hakuta K 2009 *Phys. Rev. A* **80** 053826
[7] Ding W, Andrews S R and Maier S A 2007 *Opt. Lett.* **32** 2499
[8] Yu Y, Ding W, Gan L, Li Z-Y, Luo Q and Andrews S 2014 *Opt. Express* **22** 2528
[9] Gong Y and Vukovi J 2010 *Appl. Phys. Lett.* **96** 031107
[10] Foresi J S, Villeneuve P R, Ferrera J, Thoen E R, Steinmeyer G, Fan S, Joannopoulos J D, Kimerling L C, Smith H I and Ippen E P 1997 *Nature* **390** 143
[11] Ding W, Liu R-J and Li Z-Y 2012 *Opt. Express* **20** 28641

[12] Nayak K P, Le Kien F, Kawai Y, Hakuta K, Nakajima K, Miyazaki H T and Sugimoto Y 2011 *Opt. Express* **19** 14040
[13] Wuttke C, Becker M, Brückner S, Rothhardt M and Rauschenbeutel A 2012 *Opt. Lett.* **37** 1949
[14] Ding M, Wang P-F, Lee T and Brambilla G 2011 *Appl. Phys. Lett.* **99** 051105
[15] Lalanne P, Sauvan C and Hugonin J P 2008 *Laser & Photon. Rev.* **2** 514
[16] Shen P and Palais J C 1999 *Appl. Opt.* **38** 1686
[17] Wan F, Ding W and Wang Z-Y 2006 *Chinese J. Electron.* **15** 619
[18] Karge H and Mühle R 1992 *Nuclear Instruments & Methods in Physics Research B* **65** 380
[19] Morgan J, Notte J, Hill R and Ward B 2006 *Microscopy Today* **14** 24

Corrigendum: Optical microfiber-based photonic crystal cavity

Yi-zhi Sun[1,3], Yang Yu[2], Hui-lan Liu[1], Zhi-yuan Li[2] and Wei Ding[2,3]

[1]School of Instrumentation Science and Opto-electronics Engineering, Beihang University, Beijing 100191, China
[2]Laboratory of Optical Physics, Institute of Physics, Chinese Academy of Sciences, Beijing 100190, China

CORRIGENDUM TO: Yi-zhi Sun, Yang Yu et al 2016 *J.Phys.: Conf.Ser*. **680** 012029

We would like to re-evaluate the contribution of Yi-zhi Sun and Yang Yu to this work by changing the first author of the published article. The correct list of anthors for the paper 'Optical microfiber-based photonic crystal cavity' is:

Yang Yu[1], Yi-zhi Sun[1,3], Steve Andrews[2], Zhi-yuan Li[1] and Wei Ding[1]

[1]Laboratory of Optical Physics, Institute of Physics, Chinese Academy of Sciences, Beijing 100190, China
[2]Department of Physics, University of Bath, Bath BA2 7AY, UK
[3]School of Instrumentation Science and Opto-electronics Engineering, Beihang University, Beijing 100191, China